American Mineralogist, Volume 92, pages 1232–1237, 2007

Magmatic paragonite in trondhjemites from the Sierra del Convento mélange, Cuba*

Antonio García-Casco†

Departamento de Mineralogía y Petrología, Universidad de Granada, Avda. Fuentenueva sn, 18002 Granada, Spain

Abstract

In the Sierra del Convento mélange peraluminous trondhjemitic-tonalitic rocks, formed by partial melting of subducted oceanic crust at ca. 15 kbar, 700 °C, contain millimeter-sized crystals of paragonite that appear to be of magmatic origin. These crystals are replaced by plagioclase and quartz along the rims. Chemically relict paragonite cores have high K contents (up to 0.35 apfu), whereas K is low at the rims (down to ca. 0.10 apfu). Calcium is relatively high in the cores and rims (0.06–0.11 apfu). The relict core compositions contrast significantly with small matrix paragonite crystals, which formed during subsequent subsolidus retrogression of relictic magmatic plagioclase at high pressure/low temperature (ca. 400 °C, 8 kbar). Textural relations, mineral composition, and calculations of phase relationships in the system NCASH strongly suggest that primary paragonite formed by crystallization of a silicate melt. This appears to be the first reported occurrence of magmatic paragonite.

Keywords: Magmatic paragonite, trondhjemite, mélange, subduction

Introduction

Paragonite commonly occurs in a variety of bulk compositions (including metabasites, metapelites, feldspathic gneisses, metagreywackes, calc-schists, and meta-evaporites) metamorphosed at low to high pressure and low- to medium-grade conditions (Harder 1956; Zen and Albee 1964; Guidotti 1968, 1984; Evans and Brown 1986; Carswell 1990; Guidotti et al. 1994; Guidotti and Sassi 2002). However, only a few reports have noted its occurrence in rocks metamorphosed at high temperature (>650 °C; e.g., Daczko et al. 2002; Hermann and Rubatto 2003; Keller et al. 2004), and no one has reported it as magmatic phase in migmatites and/or igneous rocks so far (Speer 1984).

Experimental and theoretical studies have established the basic subsolidus and supersolidus phase relations of mineral assemblages involving paragonite (Chatterjee 1970, 1972, 1973, 1974; Thompson 1974; Huang and Wyllie 1974; Chatterjee and Froese 1975; Thompson and Algor 1977; Holland 1979). These relations show that the subsolidus stability of paragonite in quartz-bearing rocks at moderate pressure is controlled by the reaction (NASH system):

Paragonite + Quartz = Albite + Al-silicate + H_2O.

This reaction has a positive dP/dT slope and intersects the H_2O-bearing NASH solidus at an invariant point located at ca. 8–9 kbar and 650 °C. Consequently, it follows from the theory of phase relationships that paragonite is stable above the wet solidus in appropriate bulk compositions. The wet solidus around the invariant point is defined by the eutectic reactions (e.g., Thompson and Algor 1977):

Albite + Quartz + Paragonite + H_2O = Melt (at P > 8–9 kbar), and

Albite + Quartz + Kyanite + H_2O = Melt (at P < 8–9 kbar).

This arrangement yields a lower pressure limit of magmatic paragonite of 8–9 kbar (at ca. 650 °C) in this system. Similar relations for the albite-free jadeite-bearing assemblages indicate that the high-pressure limit of supersolidus paragonite is located at another invariant point at ca. 24 kbar and ca. 700 °C. Magmatic paragonite is thus expected to occur in magmas of appropriate (hydrous, silica saturated, peraluminous, and sodium-rich) bulk compositions crystallized at great depth. The scarcity of magmatic paragonite, in consequence, may simply be due to the relatively low-pressure conditions of the crystallization of these melts.

Recently, however, trondhjemitic-tonalitic rocks formed by partial melting of garnet amphibolites and subsequently crystallized at great depth have been discovered in the subduction-related Sierra del Convento mélange in eastern Cuba (García-Casco 2005). The mélange is exceptional compared to other occurrences of oceanic subduction complexes exhumed to the Earth's surface due to the evidence of partial melting processes taking place during subduction.

Geologic setting

The Sierra del Convento mélange represents an oceanic subduction channel related to subduction of the Protocaribbean lithosphere below the Caribbean plate during the Cretaceous (García-Casco et al. 2006). It consists of a low-grade serpentinite

* This paper is dedicated to the memory of Charles Guidotti, who died on May 19, 2005, and who greatly contributed to the petrological understanding of the micas.

† E-mail: agcasco@ugr.es

matrix, which contains a variety of tectonic blocks metamorphosed under high pressure and low to high temperature, including greenschist, blueschists, pelitic gneisses, and epidote-garnet amphibolites. The formation of the mélange started in the early Cretaceous (ca. 120 Ma) and proceeded until the complex was emplaced on top of the Purial volcanic arc complex during the latest Cretaceous (García-Casco et al. 2006).

The most common rock type in the mélange is a MORB-derived plagioclase-lacking epidote ± garnet amphibolite. This rock is typically closely associated with cm- to dm-sized trondhjemitic to tonalitic segregations forming concordant layers parallel to the main syn-metamorphic foliation of the amphibolites as well as crosscutting bodies and veins. Banded, stromatic, vein-like, and agmatitic structures typical of migmatites are common. The segregations have low K_2O (0.08–0.26 wt%), FeO (0.49–1.68 wt%), and MgO (0.17–1.18 wt%) contents, but are relatively rich (0.38–0.67) in Mg no. [$Mg/(Mg + Fe_{total})$], and are peraluminous (alumina saturation index = 1.023–1.142; Table 1).

As discussed by García-Casco (2005) petrological and geochemical evidence support that the segregations formed upon wet melting of subducted tholeiitic amphibolites at 675–700 °C and 14–16 kbar. These conditions indicate hot subduction likely caused by the onset of subduction of a young oceanic lithosphere. In addition, subsequent exhumation took place in a syn-subduction scenario, allowing the blocks to follow counterclockwise *P-T* paths due to continuous cooling of the subduction system and, as a consequence, the trondhjemitic melts crystallized at great depth.

Table 1. Chemical composition of whole rock SC21 (wt%) and of primary (relict and readjusted) and retrograde (after plagioclase) paragonite [wt% and atoms per 20 O and 4 (OH,F,Cl)]

	SC21	Primary				After pl
SiO_2	60.46	46.43	45.80	45.66	46.22	47.46
TiO_2	0.22	0.17	0.28	0.25	0.21	0.10
Al_2O_3	22.30	39.06	38.87	38.48	39.28	39.70
Cr_2O_3	na	0.03	0.00	0.00	0.00	0.00
FeO_{tot}	1.68	0.39	0.38	0.42	0.42	0.21
MnO	0.03	0.02	0.00	0.00	0.01	0.00
MgO	1.18	0.26	0.21	0.24	0.23	0.35
CaO	6.01	0.42	0.45	0.41	0.61	0.22
BaO	na	0.25	0.19	0.25	0.10	0.02
Na_2O	6.45	6.25	6.33	6.14	6.71	7.31
K_2O	0.17	2.11	1.98	1.94	1.14	0.67
P_2O_5	0.05	na	na	na	na	na
F	na	0.00	0.00	0.00	0.00	0.01
Cl	na	0.01	0.01	0.00	0.01	0.02
LOI/H_2O	1.23	4.65	4.61	4.58	4.65	4.73
Total	99.78	100.05	99.11	98.39	99.59	100.79
Si		5.98	5.95	5.97	5.95	6.01
Ti		0.02	0.03	0.02	0.02	0.01
Al		5.93	5.95	5.93	5.96	5.93
Cr		0.00	0.00	0.00	0.00	0.00
Fe		0.04	0.04	0.05	0.05	0.02
Mn		0.00	0.00	0.00	0.00	0.00
Mg		0.05	0.04	0.05	0.04	0.07
Ca		0.06	0.06	0.06	0.08	0.03
Ba		0.01	0.01	0.01	0.01	0.00
Na		1.56	1.59	1.56	1.67	1.80
K		0.35	0.33	0.32	0.19	0.11
F		0.00	0.00	0.00	0.00	0.00
Cl		0.00	0.00	0.00	0.00	0.00
OH		4.00	4.00	4.00	4.00	3.99

Notes: Total Fe expressed as Fe^{2+}. H_2O (wt%) in paragonite calculated after stoichiometry. H_2O in whole-rock analysis represents weight lost on ignition. na = Not analyzed.

Analytical techinques

Whole-rock and mineral compositions (Table 1) were determined on glass beads by XRF using a PHILIPS Magix Pro (PW-2440) spectrometer and by WDS using a CAMECA SX-50 electron microprobe, respectively, at the University of Granada (see García-Casco et al. 1993, for details of routine operation conditions of the electron microprobe). X-ray distribution images were obtained on the electron microprobe using analytical conditions of 20 kV, 292 nA beam current, with step (pixel) size of 5 μm and counting times of 25 ms (Si, Al, Fe, and Ca) and 50 ms (Ti, Mg, Na, and K). I have found that high beam current combined with short counting time (milliseconds rather than seconds) avoids the problem of beam damage to silicates. These images were processed with the software *Imager* (Torres-Roldán and García-Casco, unpublished) to obtain quantitative images of paragonite composition. The procedure of Bence and Albee (1968) was followed for matrix correction by using the composition of an internal paragonite standard analyzed with the electron microprobe, the α-factor table by Kato (2005; see also http://www.nendai.nagoya-u.ac.jp/gsd/a-factor), and a correction for 3.5 μs dead time. The images of Figures 1a and 1b show these pixel-sized analyses of paragonite expressed in apfu (atoms per 22 O atoms formula unit; color code) with all other mineral phases masked out, overlain onto a grayscale base-layer showing the raw Na*K*α signal (counts/nA/s) of the matrix to show the basic textural feature of the scanned area.

Textural relations and mineral compositions

The primary (presumably magmatic) assemblage of the trondhjemitic-tonalitic segregates consists of medium grained plagioclase (X_{an} up to 0.3), quartz, epidote (Fe^{3+} ca. 0.5 atoms per 12.5 O atoms), and minor amounts of pargasitic amphibole [Si down to 6.01, Al up to 2.87, Ti up to 0.26, Na(A) up to 0.72, K(A) up to 0.11, Na(B) ca. 0.35 atoms per 23 O atoms, Mg no. ca. 0.75], paragonite, apatite, rutile, and titanite (up to 0.072 Al per 5 O atoms). Retrogression occurs and most magmatic plagioclase has largely been transformed into albite, clinozoisite, paragonite, and, locally lawsonite. Magmatic epidote shows fine-grained overgrowths of clinozoisite + quartz intergrowths, which grow from the magmatic epidote crystals into adjacent plagioclase. Magmatic pargasite is partly replaced by magnesiohornblende-tremolite, chlorite, and pumpellyite. Rutile shows titanite replacements. Occasional fine-grained phengitic mica and K-feldspar replace primary plagioclase, paragonite, and/or pargasite.

Primary paragonite occurs as medium grained crystals (2–3 mm in length, ca. 0.5 mm in width), which appear corroded, though almost idiomorphic crystals also occur. The textural description focuses on the representative sample SC21, which has primary paragonite replaced by plagioclase and quartz plus little K-feldspar because this sample nicely illustrates the magmatic as well as the subsolidus history of paragonite growth. Primary paragonite shown in Figures 1a and 1b shows patchy zoning related to later retrogression, displaying relict high-K areas (up to 0.35 apfu) and K-poorer areas (down to ca. 0.10 apfu) distributed irregularly but typically along the (001) planes and close to the crystal rims. This suggests crystallization of the crystals at high *T* (with the composition of relict core areas) and subsequent retrograde chemical readjustment during subsolidus retrogression

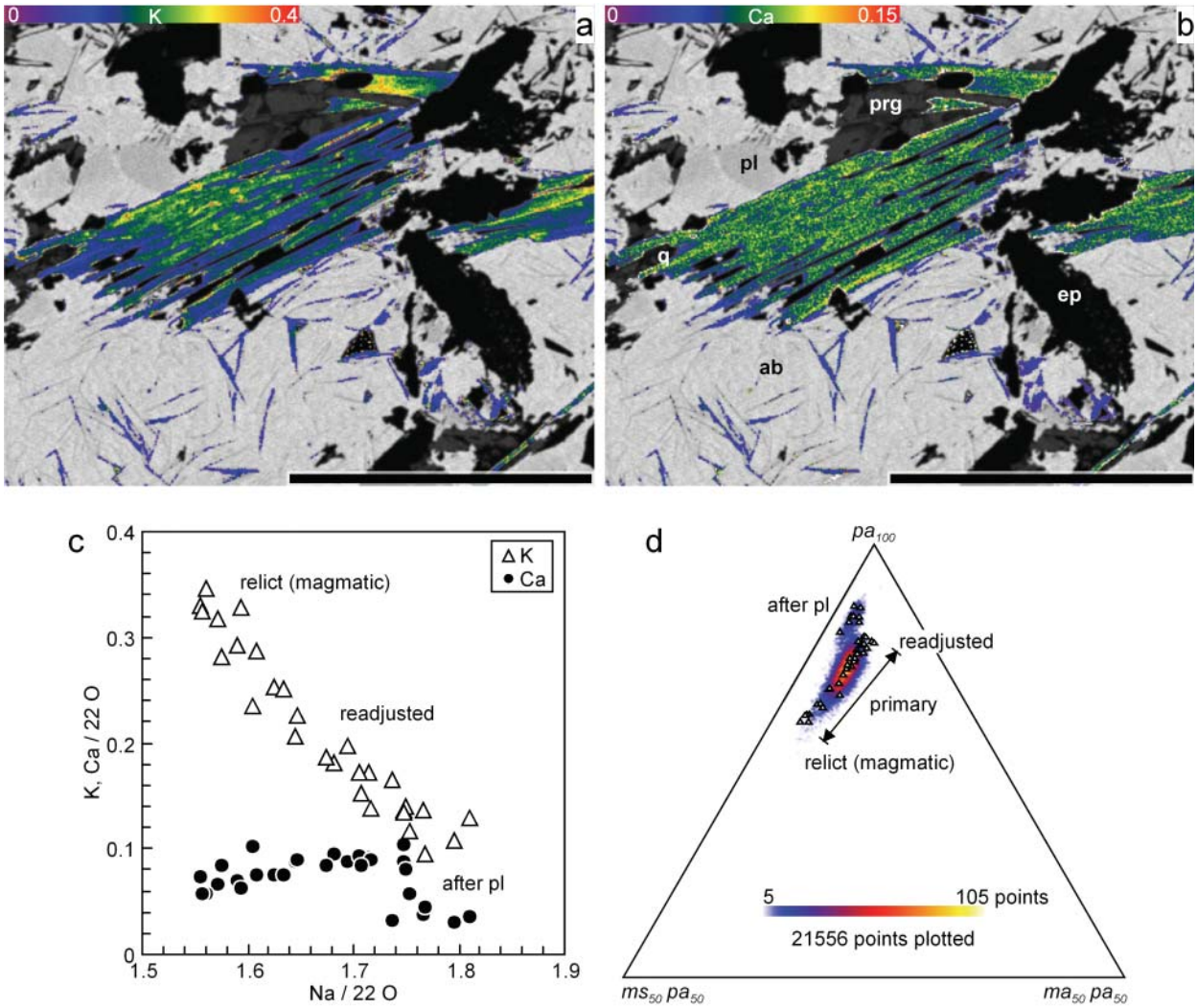

FIGURE 1. Textural and compositional features of paragonite. (**a**) K and (**b**) Ca distribution expressed in apfu in primary (large crystals) and retrograde (tiny crystals) paragonite. Quartz = q, plagioclase = pl, albite = ab, epidote = ep, pargasite = prg. Scale bar = 1 mm. (**c**) Ca and K vs. Na (apfu) of single spot analyses. (**d**) Ca-Na-K ternary with projection of single spot analyses (triangles) and quantified pixels of X-ray distribution images expressed as absolute frequency colors. See text for details.

(Figs. 1a and 1c). The concentration of Ca is relatively high in the relict high-K areas, though it increases slightly in the readjusted low-K areas (0.06–0.11 apfu, Figs. 1b and 1c). The K-Na-Ca relations indicate that the main effect of chemical readjustment can be explained with an increase in the paragonite component through the NaK_{-1} exchange and a slight increase in the margarite component through the $^{[XII]}Ca^{[IV]}Al(^{[XII]}Na^{[IV]}Si)_{-1}$ exchange vector (Fig. 1d). During subsequent subsolidus retrogression, finer grains (<0.5 mm in length) of secondary paragonite replaced magmatic plagioclase. These grains have K- and Ca-poor compositions (Figs. 1a–1d). The Ti and Fe^{2+}_{total} + Mg contents are 0–0.028 and 0.039–0.103 apfu, respectively, showing higher amounts in primary paragonite.

Primary paragonite formation at high temperature is inferred from the behavior of the paragonite-muscovite and paragonite-margarite binary phase relations and solid solutions (e.g., Chatterjee and Flux 1986; Franz et al. 1977). For example, minimum temperature of formation of the composition with the highest K/(K + Na) = 0.18 calculated using the binary paragonite-muscovite solvus model of Chatterjee and Flux (1986) is 794 and 903 °C at 10 and 15 kbar, respectively. These temperatures appear to be overestimated, perhaps due to the non-accounted effect of Ca in the thermodynamic model. Indeed, *P-T* calculations using THERMOCALC v. 3.25 (Holland and Powell 1998, data set 5.5, 12-Nov-04) give 700–650 °C and 15–12 kbar for crystallization of the trondhjemitic liquid. The same technique gives down to ca. 400 °C and 8 kbar for formation of retrograde paragonite, indicating cooling at relatively high-pressure (Fig. 2). Calculations were performed using different combinations of the composition of the phases grown during supersolidus (pargasitic Amp + Ep + high-K Pa + Qtz + high-Ca-Pl) and retrograde (tremolitic Amp + Chl + Czo + low-K Pa + Qtz +

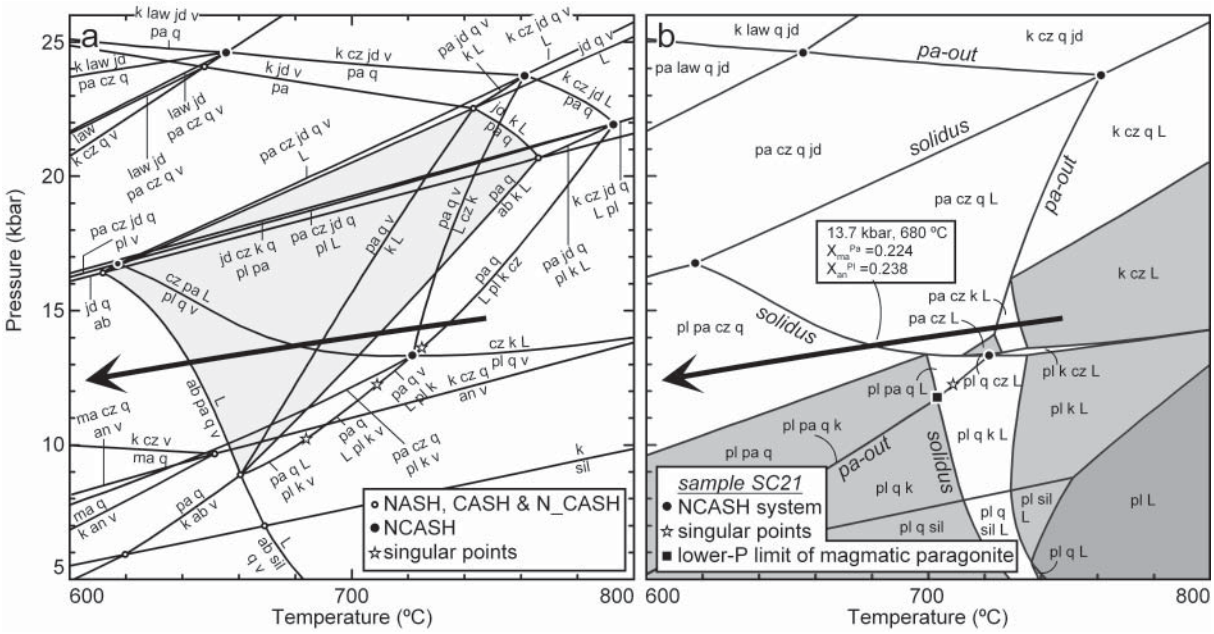

FIGURE 2. (**a**) NASH, CASH, N_CASH, and NCASH grids constructed for quartz-saturation throughout the *P-T* window considered and H_2O-saturation only for subsolidus conditions. The N_CASH and NCASH systems incorporate reactions between pure Na and pure Ca solid phases (Na-Ca solutions are not allowed) and between Na-Ca solid and liquid solutions, respectively. (**b**) H_2O-saturated NCASH pseudosection for sample SC21 (SiO_2:Al_2O_3:CaO:Na_2O = 70.07:15.23:7.46:7.24 molar units) calculated using THERMOCALC v. 3.25. The phases considered are silicate liquid (L), quartz (q), plagioclase (pl), paragonite (pa), margarite (ma), kyanite (k), sillimanite, (sil), lawsonite (law), clinozoisite (cz), jadeite (jd), and H_2O-fluid (v). The NCASH solution models for the silicate melt, plagioclase, and paragonite/margarite are according to Holland and Powell (2001), Holland and Powell (2003), and Worley and Powell (1998), respectively, modified for compositions with K = 0. The thick arrow is the calculated *P-T* path for sample SC21. The code for assemblage variance is white = 2-variant, light-gray = 3-variant, and dark-gray = 4-variant.

Ab) conditions. To keep the calculated *P-T* error ellipses small and improve the statistics of the calculations, phase components with low activities were neglected in the calculations. A H_2O-fluid was included in all assemblages.

PHASE RELATIONS INVOLVING MAGMATIC PARAGONITE

Although the phase relations (*P-T* grid) of interest in the NASH system are fairly well known, the effect of Ca in partial melting relations has not been quantitatively assessed in detail. A series of petrogenetic grids that incorporate partial melting reactions in the systems NASH, CASH, N_CASH (involving pure Na and Ca species), and NCASH (involving Na-Ca solid and liquid solutions) have been developed using THERMOCALC v. 3.25 (Fig. 2a). The solution models used for silicate melt in the various systems incorporate a "sillimanite" component to account for the peraluminous composition of the trondhjemitic-tonalitic melts of the Sierra del Convento.

Magmatic paragonite (+ quartz) has a maximum *P-T* window of stability of 8.5–23 kbar and 610–760 °C in the NASH grid (Fig 2a), fully consistent with previously developed NASH grids. The stability of paragonite is shifted to higher temperature and pressure in the NCASH system. Because partial melting was fluid-assisted, the pseudosection for sample SC21 (Fig. 2b) was constructed for H_2O-saturated conditions. Even if these conditions do not prevail during the full *P-T* range of interest (because of the high solubility of H_2O in silicate melt at high pressures), the calculated phase relations fit well with observed assemblages in the region close to the solidus. The pseudosection predicts magmatic paragonite and clinozoisite to coexist along the near isobaric cooling path deduced for this sample. At the H_2O-saturated NCASH solidus, magmatic paragonite reacts with the residual liquid (and clinozoisite) to form plagioclase and quartz along the reaction:

$$\text{Paragonite} + \text{Clinozoisite} + \text{Melt} = \text{Plagioclase} + \text{Quartz} + H_2O$$

but residual magmatic paragonite would persist upon liquid exhaustion (i.e., below the solidus). These predictions are consistent with the observed corrosion of primary paragonite by plagioclase and quartz in sample SC21 (Figs. 1a and 1b) and with subsequent growth of subsolidus paragonite. Also, the composition of magmatic plagioclase and paragonite are predicted to be relatively rich in Ca at the calculated conditions of intersection of the solidus (13.7 kbar, 680 °C, X_{ma}^{Pa} =0.224; X_{an}^{Pl} =0.238, Fig. 2b) in agreement with the compositions of relict plagioclase and paragonite of sample SC21.

DISCUSSION

As compared to other moderate to high-temperature occurrences of paragonite, primary paragonite in the Sierra del Convento trondhjemites appears to have the highest K-contents ever reported, i.e., up to 0.35 apfu (in sample SC21) vs. 0.2 apfu of subsolidus paragonite formed at 600–700 °C, 12–14 kbar (Daczko et al. 2002) and 0.24 apfu of paragonite in sillimanite-bearing schist formed at 500–550 °C, 3.7–4.7 kbar (Grambling 1984). These figures strengthen the conclusion of a magmatic

character of the studied paragonite crystals.

Formation of paragonite has been inferred to occur at high temperatures (>600 °C) in intermediate to high-pressure rocks of mafic, quartz-feldspathic, and pelitic compositions (Daczko et al. 2002; Hermann and Rubatto 2003; Keller et al. 2004), and it has been considered to be a reactant phase in melt-forming reactions at >700 °C (e.g., Hermann and Rubatto 2003). However, it has not been reported as a product of magmatic crystallization so far. The phase relations depicted in Figures 2a and 2b indicate that magmatic paragonite is not stable at pressures below 8 kbar. Thus, it can be concluded that the scarcity of magmatic paragonite in appropriate natural rocks crystallized from melts is the consequence of decompression-dominated *P-T* paths of ascending trondhjemitic-tonalitic magmas. In these systems, the fate of magmatic paragonite eventually formed at deep-seated conditions is to react out (and thus produce kyanite and more melt) as the system decompresses. Only special conditions, such as near-isobaric cooling at >8 kbar similar to the one followed by the trondhjemites of the Sierra del Convento mélange would prevent magmatic paragonite to disappear.

The composition of melts appropriate for formation of magmatic paragonite should be hydrous, silicic, K-poor, Na-rich, and peraluminous. Of these features, peraluminosity is an important control for the formation of magmatic paragonite in a similar way as it does control the formation of magmatic muscovite in K-rich granitic melts/magmas (crystallized at pressures higher than ca. 4 kbar). While peraluminosity in granitic magma is readily explained by partial melting of peraluminous terrigenous sources, the peraluminous character of trondhjemitic-tonalitic magmas formed after melting of metaluminous metabasite compositions is debated (e.g., Johannes and Holtz 1996). However, several experimental studies have firmly established that partial melting of metaluminous metabasite produces peraluminous melts under both water-saturated and water-undersaturated conditions (e.g., Helz 1976; Ellis and Thompson 1986; Beard and Lofgren 1991; Thompson and Ellis 1994; Patiño Douce and Beard 1995; Rapp and Watson 1995). Thus, it appears that primary tonalite-trondhjemite melts formed after partial melting of metabasite can be peraluminous and crystallize peraluminous minerals, as in the Sierra del Convento mélange. The lack of this character in evolved magmas may be explained by post-melting modification during assimilation and/or fractional crystallization and/or magma mixing processes, which occur during the protracted supersolidus histories of magmatic rocks.

Acknowledgments

The author thanks W. Gary Ernst and Peter Tropper for their reviews and comments. The assistance of Guillermo Millán, Kenya Núñez, and Antonio Rodríguez Vega during field work is acknowledged. This research was supported by Spanish MEC grants BTE 2002-01011 and CGL2006-08527 to the University of Granada.

References cited

Beard, J.S. and Lofgren, G.E. (1991) Dehydration melting and water-saturated melting of basaltic and andesitic greenstones and amphibolites at 1, 3, and 6.9 kb. Journal of Petrology, 32, 365–401.

Bence, A.E. and Albee, A.L. (1968) Empirical correction factors for the electron microanalysis of silicate and oxides. Journal of Geology, 76, 382–403.

Carswell, D.A., Ed. (1990) Eclogite-facies rocks, 396 p. Blackie, Glasgow.

Chatterjee, N.D. (1970) Synthesis and upper stability of paragonite. Contributions to Mineralogy and Petrology, 27, 244–257.

——— (1972) The upper stability limit of the assemblage paragonite + quartz and its natural occurrences. Contributions to Mineralogy and Petrology, 31, 288–303.

——— (1973) Low-temperature compatibility relations of the assemblage quartz-paragonite and the thermodynamic status of the phase rectorite. Contributions to Mineralogy and Petrology, 42, 259–271.

——— (1974) Crystal-liquid-vapour equilibria involving paragonite in the system $NaAlSi_3O_8$-Al_2O_3-SiO_2-H_2O. Indian Journal of Earth Sciences, 1, 3–11.

Chatterjee, N.D. and Flux, S. (1986) Thermodynamic mixing properties of muscovite-paragonite crystalline solutions at high temperatures and pressures, and their geological applications. Journal of Petrology, 27, 677–693.

Chatterjee, N.D. and Froese, E. (1975) A thermodynamic study of the pseudobinary join muscovite–paragonite in the system $KAlSi_3O_8$-$NaAlSi_3O_8$-Al_2O_3-SiO_2-H_2O. American Mineralogist, 60, 985–993.

Daczko, N.R., Clarke, G.L., and Klepeis, K.A. (2002) Kyanite-paragonite-bearing assemblages, northern Fiordland, New Zealand: rapid cooling of the lower crustal root to a Cretaceous magmatic arc. Journal of Metamorphic Geology, 20, 887–902.

Evans, B.W. and Brown, E.H., Eds. (1986) Blueschists and eclogites, 423 p. Geological Society of America Memoir 164, Boulder, Colorado.

Ellis, D.J. and Thompson, A.B. (1986) Subsolidus and partial melting reactions in the quartz-excess $CaO+MgO+Al_2O_3+SiO_2+H_2O$ system under water-excess and water deficient conditions to 10 kb: Some implications for the origin of peraluminous melts from mafic rocks. Journal of Petrology, 27, 91–121.

Franz, G., Hinrichsen, T., and Wannemacher, E. (1977) Determination of the miscibility gap on the solid solution series paragonite-margarite by means of the infrared spectroscopy. Contributions to Mineralogy and Petrology, 59, 307–316.

García-Casco, A. (2005) Partial melting and counter-clockwise *P-T* path of subducted oceanic crust: a case study of hot subduction in the northern Caribbean (E Cuba). In Metamorphic Studies Group, Keynote address, 1–2. Research in Progress and Annual General Meeting, The Geological Society, London, March 2005, http://msg.gly.bris.ac.uk/pages/mpages/rip05.html.

García-Casco, A., Sánchez-Navas, A., and Torres-Roldán, R.L. (1993) Disequilibrium decomposition and breakdown of muscovite in high *P-T* gneisses, Betic alpine belt (southern Spain). American Mineralogist, 78, 158–177.

García-Casco, A., Torres-Roldán R.L., Iturralde-Vinent, M.A., Millán, G., Núñez, K., Lázaro, C., and Rodríguez Vega, A. (2006) High pressure metamorphism of ophiolites in Cuba. Geologica Acta, 4, 63–88.

Grambling, J.A. (1984) Coexisting paragonite and quartz in sillimanitic rocks from New Mexico. American Mineralogist, 69, 79–87.

Guidotti, C.V. (1968) On the relative scarcity of paragonite. American Mineralogist, 53, 963–974.

——— (1984) Micas in metamorphic rocks. In S.W. Bailey, Ed., Micas, 13, p. 357–467. Reviews in Mineralogy, Mineral Society of America, Chantilly, Virginia.

Guidotti, C.V. and Sassi, F.P. (2002) Constraints on studies of metamorphic K-Na white micas. In A. Mottana, F.P. Sassi, J.B. Thompson, and S. Guggenheim, Eds., Micas: Crystal chemistry and metamorphic petrology, 46, p. 413–448. Reviews in Mineralogy and Geochemistry, Mineral Society of America, Chantilly, Virginia.

Guidotti, C.V., Sassi, F.P., Blencoe, J.G., and Selverstone, J. (1994) The paragonite-muscovite solvus. I. *P-T-X* limits derived from the Na-K compositions of natural, quasibinary paragonite-muscovite pairs. Geochimica et Cosmochimimica Acta, 58, 2269–2275.

Harder, H. (1956) Untersuchungen an Paragoniten und an natriumhaltigen Muskoviten. Heidelberger Beitraege zur Mineralogie und Petrologie, 5, 227–271.

Helz, R.T. (1976) Phase relations of basalt in their melting ranges at P_{H2O} = 5 kb. Part II. Melt compositions. Journal of Petrology, 17, 139–193.

Hermann, J. and Rubatto, D. (2003) Relating zircon and monazite domains to garnet growth zones: age and duration of granulite facies metamorphism in the Val Malenco lower crust. Journal of Metamorphic Geology, 21, 833–852.

Holland, T.J.B. (1979) Experimental determination of the reaction paragonite = jadeite + kyanite + H_2O, and internally consistent thermodynamic data for part of the system Na_2O-Al_2O_3-SiO_2-H_2O, with applications to eclogites and blueschists. Contributions to Mineralogy and Petrology, 68, 293–301.

Holland, T.J.B. and Powell, R. (1998) An internally consistent thermodynamic data set for phases of petrological interest. Journal of Metamorphic Geology, 16, 309–343.

——— (2001) Calculation of phase relations involving haplogranitic melts using an internally consistent thermodynamic data set. Journal of Petrology, 42, 673–683.

——— (2003) Activity-composition relations for phases in petrological calculations: an asymmetric multicomponent formulation. Contributions to Mineralogy and Petrology, 145, 492–501.

Huang, W.L. and Wyllie, P.J. (1974) Melting relations of muscovite with quartz and sanidine in the K_2O-Al_2O_3-SiO_2-H_2O system to 30 kbars and an outline of paragonite melting reactions. American Journal of Science, 274, 378–395.

Johannes, W. and Holtz, F. (1996) Petrogenesis and experimental petrology of granitic rocks, 335 p. Springer, Berlin.

Kato, T. (2005) New accurate Bence-Albee α-factors for oxides and silicates calculated from the PAP correction procedure. Geostandards and Geoanalytical Research, 29, 83–94.

Keller, L.M., Abart, R., Stünitz, H., and De Capitani, C. (2004) Deformation, mass

transfer and mineral reactions in an eclogite facies shear zone in a polymetamorphic metapelite (Monte Rosa nappe, western Alps). Journal of Metamorphic Geology, 22, 97–118.
Patiño Douce, A.E. and Beard, J.S. (1995) Dehydration melting of biotite gneiss and quartz amphibolite from 3 to 15 kbar. Journal of Petrology, 36, 707–738.
Rapp, R.P. and Watson, E.B. (1995) Dehydration melting of metabasalt at 8–32 kbar: Implications for continental growth and crust-mantle recycling. Journal of Petrology, 36, 891–931.
Speer, J.A. (1984) Micas in igneous rocks. In S.W. Bailey, Ed., Micas, 13, p. 229–356. Reviews in Mineralogy, Mineral Society of America, Chantilly, Virginia.
Thompson, A.B. (1974) Calculation of muscovite-paragonite-alkali feldspar phase relations. Contributions to Mineralogy and Petrology, 44, 173–194.
Thompson, A.B. and Algor, J.R. (1977) Model system for anatexis of pelitic rocks. I. Theory of melting reactions in the system $KAlO_2$-$NaAlO_2$-Al_2O_3-SiO_2-H_2O. Contributions to Mineralogy and Petrology, 63, 247–269.
Thompson, A.B. and Ellis, D.J. (1994) CaO+MgO+Al_2O_3+SiO_2+H_2O to 35 kb: Amphibole, talc, and zoisite dehydration and melting reactions in the silica-excess part of the system and their possible significance in subduction zones, amphibole melting, and magma fractionation. American Journal of Science, 294, 1229–1289.
Worley, B. and Powell, R. (1998) Singularities in NCKFMASH (Na_2O-CaO-K_2O-FeO-MgO-Al_2O_3-SiO_2-H_2O). Journal of Metamorphic Geology, 16, 169–188.
Zen, E-an and Albee, A. (1964) Coexisting muscovite and paragonite in pelitic schists. American Mineralogist, 49, 964–925.

Manuscript received February 5, 2007
Manuscript accepted April 20, 2007
Manuscript handled by Bryan Chakoumakos